

Article

Quantitative Changes in Muscular and Capillary Oxygen Desaturation Measured by Optical Sensors during Continuous Positive Airway Pressure Titration for Obstructive Sleep Apnea

Zhongxing Zhang ^{1,2,*} , Ming Qi ¹ , Gordana Hügli ¹  and Ramin Khatami ^{1,2,3}

¹ Center for Sleep Medicine, Sleep Research and Epileptology, Clinic Barmelweid AG, 5017 Barmelweid, Switzerland; ming.qi@barmelweid.ch (M.Q.); gordana.huegli@barmelweid.ch (G.H.); ramin.khatami@barmelweid.ch (R.K.)

² Barmelweid Academy, Clinic Barmelweid AG, 5017 Barmelweid, Switzerland

³ Department of Neurology, Inselspital, Bern University Hospital, University of Bern, 3010 Bern, Switzerland

* Correspondence: zhongxing.zhang@barmelweid.ch

Abstract: Obstructive sleep apnea (OSA) is a common sleep disorder, and continuous positive airway pressure (CPAP) is the most effective treatment. Poor adherence is one of the major challenges in CPAP therapy. The recent boom of wearable optical sensors measuring oxygen saturation makes at-home multiple-night CPAP titrations possible, which may essentially improve the adherence of CPAP therapy by optimizing its pressure in a real-life setting economically. We tested whether the oxygen desaturations (ODs) measured in the arm muscle (arm_OD) by gold-standard frequency-domain multi-distance near-infrared spectroscopy (FDMD-NIRS) change quantitatively with titrated CPAP pressures in OSA patients together with polysomnography. We found that the arm_OD ($2.08 \pm 1.23\%$, mean \pm standard deviation) was significantly smaller (p -value < 0.0001) than the fingertip OD (finger_OD) ($4.46 \pm 2.37\%$) measured by a polysomnography pulse oximeter. Linear mixed-effects models suggested that CPAP pressure was a significant predictor for finger_OD but not for arm_OD. Since FDMD-NIRS measures a mixture of arterial and venous OD, whereas a fingertip pulse oximeter measures arterial OD, our results of no association between arm_OD and finger_OD indicate that the arm_OD mainly represented venous desaturation. Arm_OD measured by optical sensors used for wearables may not be a suitable indicator of the CPAP titration effectiveness.

Keywords: obstructive sleep apnea; continuous positive airway pressure therapy; near-infrared spectroscopy; oxygen desaturation; arm; pulse oximeter; wearable



Citation: Zhang, Z.; Qi, M.; Hügli, G.; Khatami, R. Quantitative Changes in Muscular and Capillary Oxygen Desaturation Measured by Optical Sensors during Continuous Positive Airway Pressure Titration for Obstructive Sleep Apnea. *Biosensors* **2022**, *12*, 3.
<https://doi.org/10.3390/bios12010003>

Received: 28 October 2021

Accepted: 19 December 2021

Published: 21 December 2021

Publisher's Note: MDPI stays neutral with regard to jurisdictional claims in published maps and institutional affiliations.



Copyright: © 2021 by the authors. Licensee MDPI, Basel, Switzerland. This article is an open access article distributed under the terms and conditions of the Creative Commons Attribution (CC BY) license (<https://creativecommons.org/licenses/by/4.0/>).

1. Introduction

Obstructive sleep apnea (OSA) is the most prevalent respiratory sleep disorder, occurring in 9–38% of the general population [1], and it is a high-risk factor for many diseases, such as cardio-/cerebrovascular diseases [2,3], periodontal disease [4] and type 2 diabetes [5]. Although different treatments (e.g., oral appliances, such as mandibular advancement devices, or other treatments, such as positional therapy, uvulopalatopharyngoplasty and hypoglossal nerve stimulation) [6] are available, continuous positive airway pressure (CPAP) or automatic positive airway pressure (APAP) therapy is currently the most effective treatment for OSA [7,8]. However, there are still many challenges in OSA diagnosis and treatment, particularly simple low-cost new diagnostic technologies that can be easily used by the patients for home recordings are urgently needed [9,10]. This urgency is due to observations that: (1) the majority of suspected OSA patients remain undiagnosed in many countries due to the lack of sleep laboratories/specialists, the little diagnostic value of daytime sleepiness for most people and the high cost of in-lab polysomnography (PSG) diagnosis [11–13]; and (2) long-term home recordings employing these easy-to-use technologies will be helpful to longitudinally monitor the CPAP treatment effects and

adherence or even to select patients who will benefit most from treatment (i.e., precision or personalized medicine) [9,14].

Recently, low-cost wearable devices, such as smartwatches (e.g., the new products from Fitbit [15], Garmin [16], Huami [17] and Huawei [18]) and armbands (e.g., Humon [19,20], Moxy [21,22], Artinis [23] and Biofourmis [24]), have implemented the function of measuring peripheral capillary (SpO₂) or muscle tissue (StO₂) oxygen saturation at the arm or wrist using near-infrared light, making them possible alternatives for at-home OSA measurement. Unlike the in-lab PSG fingertip pulse oximetry, in which the detector measures the light transmitted through the fingertip (i.e., transmission photoplethysmography (T-PPG)), these wearable devices assess the SpO₂ or StO₂ by measuring the changes in the backscattering light from the wrist or arm based on the modified Beer–Lambert law (MBLL) [25–28]. That is, their light sources are usually two or more near-infrared light wavelengths mainly absorbed by oxygenated hemoglobin (HbO₂) and deoxygenated hemoglobin (HHb) in biological tissues, and detectors are placed on the same side of the measured tissues because the wrist and arm are too thick to be penetrated by light. While wrist wearable devices mainly use reflectance photoplethysmography (R-PPG) or pulse oximetry [28–30], armbands are mainly based on simple continuous-wave near-infrared spectroscopy (CW-NIRS) methods [20,22].

Measuring OSA by these low-cost wearable devices is unfortunately still not viable because none of them has been licensed or certified as a medical diagnostic device by the United States Food and Drug Administration or CE marking [31]. In our recent study [32], we compared event-by-event oxygen desaturation (OD) at the fingertip (finger_OD) measured by gold-standard in-lab PSG fingertip T-PPG with the OD at arm (arm_OD) measured by gold-standard frequency-domain multi-distance near-infrared spectroscopy (FDMD-NIRS) in OSA patients during naïve sleep and during CPAP titrations. Our Bland–Altman plots yielded poor agreement between finger_OD and arm_OD in sleep hypopneas, suggesting that the absolute value of arm_OD is not suitable to define sleep hypopneas according to the standard clinical criterion of $\geq 3\%$ OD drop. It could lead to large false-negative results in measuring OSA events, thus underestimating the Apnea–Hypopnea index (AHI) compared to in-lab PSG.

However, whether the changes in arm_OD can indicate the effectiveness of CPAP titration remains unknown. The CPAP/APAP machine itself can measure the AHI, although its accuracy has been criticized [33–35]. Two major challenges in CPAP/APAP treatment are poor adherence to treatment [36] and persisting hypoxemia and daytime syndromes despite therapy in some patients, for whom oxygen supplementation may be needed [9]. Logically, ‘A does not equal to B’ does not necessarily mean that ‘changes in A are not associated with changes in B’. For example, obesity is a risk factor for OSA. A high BMI cannot be used to replace a high AHI to define OSA, but the decrease in the BMI is associated with a decrease in the AHI [37]. If the changes in arm_OD can be associated with changes in CPAP/APAP pressures, then measuring changes in arm_OD with a wearable device at home could be helpful to better understand those patients, e.g., to identify subgroups with/without improvement in OD when CPAP/APAP pressure changes. It could also make at-home multiple-night CPAP titrations possible, i.e., to find the optimal CPAP pressure that can at best restore the respiratory events and arm_OD, which may essentially improve the adherence of CPAP therapy by optimizing its pressures in a real-life setting economically.

Therefore, in this study, we quantified the dynamic changes in arm_OD in OSA events under titrated CPAP pressures using regression analysis. We used the same dataset that has been recently published in [32], considering its major advantages, which include: (1) the CPAP pressures were well-controlled stepwise and increased hourly during titration; (2) the simultaneously measured finger_OD can serve as a control for CPAP titration effectiveness, i.e., an effective titration procedure should restore stepwise the fingertip SpO₂ desaturation; (3) the comparisons between finger_OD (i.e., arterial desaturation) and arm_OD (i.e., the mixture of arterial and venous desaturation [38,39]) may provide new insights into the peripheral desaturation in response to OSA events during CPAP therapy.

We hypothesized that the changes in arm_OD may be associated with changes in CPAP pressures, considering that our stepwise incremental CPAP titration gradually opened the upper airway to increase oxygen supply.

2. Materials and Methods

2.1. Study Design

Thirty newly diagnosed OSA patients (age (mean \pm standard deviation, SD): 54.2 ± 13.8 years, interquartile range (IQR) 42–65 years; male: $n = 27$; body mass index (BMI): 35.9 ± 7.5 kg/m², IQR 31.8–42.0 kg/m²; AHI: 53.4 ± 24.7 per hour, IQR 32–71 per hour) participated in this study. Patients with unstable coronary or cerebral artery disease, severe arterial hypertension or hypotension, respiratory diseases or a history of a sleep-related accident were excluded from this study. This study was approved by the local ethical commission of Northwest Switzerland and was in compliance with the Declaration of Helsinki. Written informed consent was obtained from all patients prior to their participation.

Patients underwent incremental stepwise CPAP (AirSense™10, ResMed) titration combined with video-PSG and FDMD-NIRS recordings in one nocturnal sleep episode. This sleep episode consisted of 1 h of baseline sleep without CPAP followed by incremental stepwise titration of 1 cmH₂O pressure per hour starting from 5–8 cmH₂O depending on the individuals. Video-PSG (Embla RemLogic, Natus Medical Incorporated, Tonawanda, NY, USA) is a comprehensive recording of physiological signals during sleep, including electroencephalography, electrooculogram, electromyogram, electrocardiogram, breathing functions, heart rate (HR), fingertip SpO₂ and movement during sleep. Two experienced sleep technologists independently scored the sleep stages, respiratory events (sleep apneas and hypopneas) and motion artifacts in 30 s epochs according to the 2017 American Academy of Sleep Medicine manual [40]. The discrepancy between these two technologists was resolved by discussion or recommendation by an experienced neurophysiologist.

FDMD-NIRS (Imagent, ISS, Champaign, IL, USA) measurements were conducted over the middle of the left biceps muscle. Imagent is currently the only commercial benchtop FDMD-NIRS device [41–43] and has been CE-approved for research. The robustness, precision and accuracy of measuring hemodynamics of the Imagent system have been well validated in different physical blood-lipid models [42,44,45] and in vivo studies [46–49]. It has been used as a gold-standard reference measurement of StO₂ for the validations or calibrations of wearable CW-NIRS armbands [20] and portable CW-NIRS oximeters including those that have received FDA clearance [45,50]. Its light emitters, four laser diodes at 690 nm wavelength and four laser diodes at 830 nm wavelength are coupled into four light sources and are high-frequency-modulated at 110 MHz. The light can penetrate into the measured tissues with a depth of several centimeters when the four light sources are aligned and placed at 2 cm, 2.5 cm, 3 cm and 3.5 cm from an optical fiber bundle connected to the photomultiplier tube detector. The sampling rate of FDMD-NIRS recording was set as 5.2 Hz. The Imagent system was calibrated on an optical phantom block to exclude the uncertainty of measurements due to machine errors before each recording. The raw measured NIRS data were subjected to a low-pass (<0.08 Hz) zero-phase filter designed using a Hanning window to remove the physiological noises including heart rate, respiratory noise and spontaneous slow hemodynamic oscillations [32,51,52]. The filtered data were then smoothed using the robust locally weighted scatter plot smoothing method [51,53].

2.2. Statistical Analysis

The data analysis procedure is shown in Figure 1. After a standard PSG scoring, per-hour AHI under each CPAP pressure was calculated, i.e., the number of events was divided by the sleep duration under each CPAP pressure per hour in the titration protocol. Obstructive apneas ($n = 29$) and hypopneas ($n = 31$) were excluded from analysis if their SpO₂ desaturations were greater than 15% to exclude outliers and potentially unreliable measurements caused by instrument errors [30,32]. In each patient, all the events under

a specific CPAP pressure were also excluded if the corresponding sleep duration under that pressure was shorter than 20 min to exclude the unreliable calculation of the per-hour AHI. For example, if the sleep duration under some CPAP pressure was just a few minutes while the patient had a number of apneas/hypopneas, the calculated per-hour AHI could be extremely large, but its value was unreliable due to short sleep duration. Then linear mixed-effects model (LMM) with a random intercept by patients was used to predict the arm_OD and finger_OD caused by the respiratory events, respectively. Explanatory variables were demographic variables (i.e., age, sex, BMI, AHI of the diagnostic night measured by PSG) and parameters that can be measured by CPAP machine or wearable devices, i.e., types of respiratory events, durations of event, sleep stages, mean HR during the events, per-hour AHI under each pressure and CPAP pressures. Stepwise regression using backward elimination was performed to automatically select the best predictors. Then the final LMM models were built using these best predictors. We reported both the conditional R^2 [54] and Ω^2 (i.e., Xu's R^2 calculated as $1 - \text{variance of residual} / \text{variance of response}$) [55] to assess the goodness of fit of our final selected models.

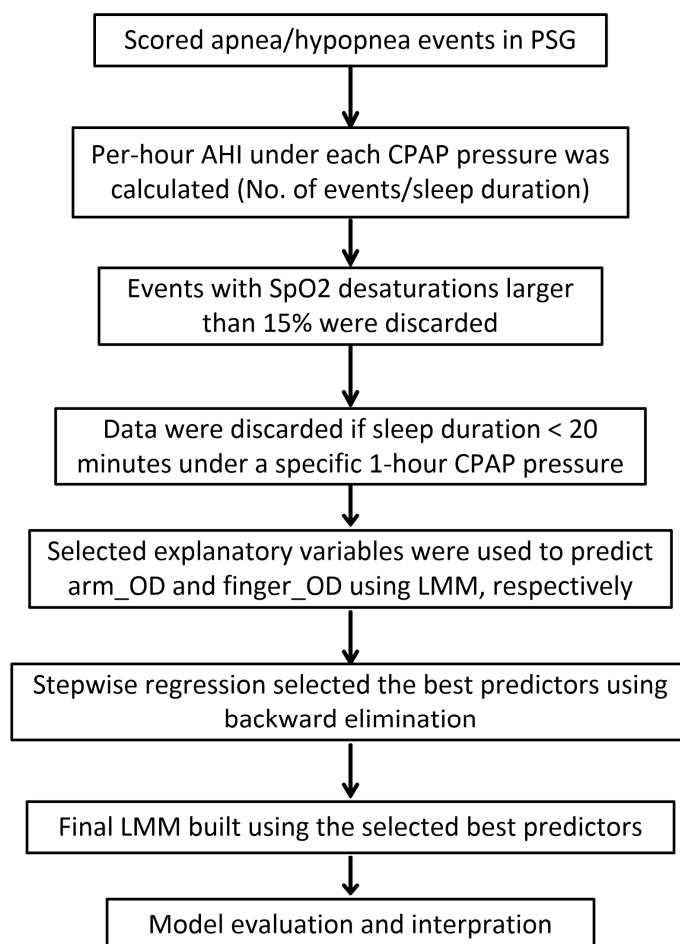


Figure 1. Data analysis procedure.

Data were expressed as the mean \pm SD unless otherwise indicated. The pre-processing of FDMD-NIRS signals was carried out in MATLAB (The MathWorks, Inc., Natick, MA, USA). All statistical analyses were performed using R (version 3.2.4). The LMM models were created using the R package *lme4* (function *lmer*) and stepwise regressions were performed using the R package *lmerTest* (function *step*).

3. Results

In total, 505 obstructive apnea and 2185 hypopnea events were analyzed. The median of the number of events acquired from our patients was 75 with an IQR between 59 and 110. Figure 2 illustrates typical changes in fingertip SpO₂ and arm StO₂ desaturations in OSA events. ODs triggered by sleep apneas occurred in both SpO₂ and StO₂, although the baseline StO₂ values (mostly between 60 and 70%) were smaller than SpO₂ (mostly above 90%) because StO₂ was from both venous and arterial blood. The mean arm_OD ($2.08 \pm 1.23\%$) was significantly smaller (paired *t*-test, *p*-value < 0.0001) than the mean finger_OD ($4.46 \pm 2.37\%$). There was no correlation between the degrees of arm_OD and finger_OD, indicated by the Pearson's correlation coefficient of 0.08 (*p*-value < 0.0001).

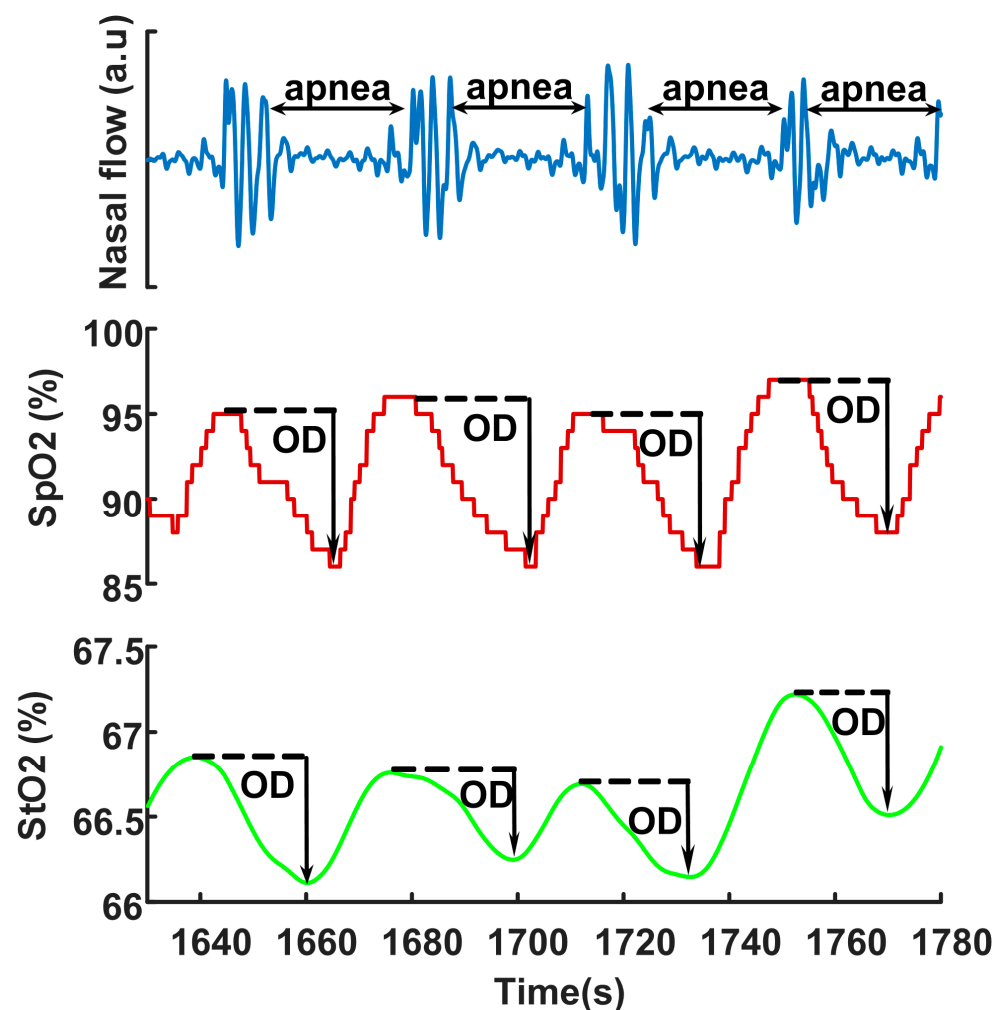


Figure 2. Typical fingertip SpO₂ desaturation and arm StO₂ desaturation during apneas. The arrow indicates the degree of oxygen desaturation (OD). SpO₂ is measured at PSG fingertip by transmission photoplethysmography, and StO₂ is measured at biceps muscle by FDMD-NIRS.

The results of the final LMMs predicting arm_OD and finger_OD selected by stepwise regressions are shown in Tables 1 and 2, respectively. The conditional R^2 and Ω^2 of the model for arm_OD were 0.66 and 0.69, respectively. These two values of the model for finger_OD were 0.51 and 0.49, respectively. CPAP pressure was a significant predictor for the finger_OD (i.e., the increase of one unit pressure was associated with 0.12% less decrease in fingertip oxygen desaturation) but not for arm_OD.

Table 1. The results of the linear mixed-effects model predicting the degree of oxygen desaturation measured at arm muscle.

	Estimate (10 ⁻²)	95% CI (10 ⁻²)	t-Value	p-Value
Duration of event	2.33	[2.00, 2.66]	13.89	<0.0001
Mean HR within events	-1.49	[-2.14, -0.84]	-4.50	<0.0001
Per-hour AHI	0.12	[0.025, 0.22]	2.47	0.014

CI: Confidence interval. HR: Heart rate. Per-hour AHI is the number of apnea/hypopnea events divided by the sleep duration under each CPAP pressure per hour.

Table 2. The results of the linear mixed-effects model predicting the degree of oxygen desaturation measured at fingertip.

	Estimate (10 ⁻²)	95% CI (10 ⁻²)	t-Value	p-Value
Duration of event	7.83	[7.01, 8.66]	18.68	<0.0001
CPAP pressures	-12.12	[-13.93, -10.31]	-13.10	<0.0001
Hypopnea–Apnea	-115.6	[-134.9, -96.3]	-11.71	<0.0001
Per-hour AHI	1.42	[1.14, 1.70]	9.87	<0.0001
Sleep stages				
Deep sleep–light sleep	-68.82	[-89.56, -48.08]	-6.51	<0.0001
REM sleep–light sleep	-56.41	[-82.13, -30.69]	-4.30	<0.0001
AHI of diagnostic night	1.93	[0.35, 3.50]	2.39	0.024

CI: Confidence interval. CPAP: Continuous positive airway pressure. REM: Rapid eye movement sleep. Per-hour AHI is the number of apnea/hypopnea events divided by the sleep duration under each CPAP pressure per hour. Hypopnea–Apnea means the change in apnea is the reference for the change in hypopnea in this model, i.e., the changes in hypopnea minus the changes in apnea. Non-rapid eye movement light sleep (stage N1 and N2) is the reference for deep sleep (stage N3) and REM sleep.

It could be possible that the normalized changes rather than the raw values of arm_OD were associated with CPAP pressures since the StO₂ baseline level ($68.6 \pm 6.4\%$) before the desaturations was obviously much smaller than that of SpO₂ (usually above 90%). We, therefore, normalized the arm_OD to its baseline and repeated the LMM analysis. The CPAP pressure was still automatically excluded from the final selected model in stepwise regression, in which the final selected predictors were the same as shown in Table 1, i.e., the duration of events (estimated coefficient 0.033, p -value < 0.0001), mean HR within events (estimated coefficient -0.03, p -value < 0.0001) and per-hour AHI (estimated coefficient 0.0028, p -value = 0.00058).

4. Discussion

In this study, we tested whether oxygen desaturations measured in the arm muscle change with CPAP pressures during CPAP titration in patients with OSA. In contrast to our recent study testing the agreement between arm and fingertip oxygen desaturations in sleep hypopneas using Bland–Altman plots [32], here we used linear regression (i.e., LMM) to study the association between CPAP pressures and oxygen desaturations at arm and fingertip. Contrary to our hypothesis, we only found association between CPAP pressures and the oxygen desaturations at the fingertip but not in the arm muscle. Our negative results suggest that muscular oxygen desaturation may be not a suitable indicator of the effectiveness of CPAP titration. Thus, the usefulness of wearable devices measuring arm StO₂ in CPAP therapy is questionable.

Only fingertip SpO₂ but not the arm StO₂ reflects the reduction of desaturations during CPAP titration, probably because venous blood contributing to StO₂ reduces the sensitivity of StO₂ in response to CPAP pressures compared to SpO₂. The NIRS StO₂ is the proportion of HbO₂ in the measured biological tissues including arterial, capillary and venous compartments. It can be expressed as:

$$\text{StO}_2 = a \times \text{SaO}_2 + b \times \text{SvO}_2 \quad (1)$$

where SaO_2 and SvO_2 are the arterial and venous oxygen saturation [38,39]. SaO_2 is approximately equal to SpO_2 as they are both arterial oxygen saturation (usually close to 100%). SvO_2 is usually 65–75% [56]. The ratio of coefficients a/b is the arterial-to-venous volume ratio (AVR), and $a + b = 1$. Most commercially available NIRS oximeters including the FDA-certificated medical devices usually fix the AVR as either 25%/75% or 30%/70% [57–67] but never validate them in OSA. If we assume that the fixed AVR model was valid in OSA, we could expect that arm_OD highly correlates with $finger_OD$ considering their mathematical relationship, e.g., a 1% decrease in fingertip arterial SpO_2 may correspond to a 0.25% or 0.3% decrease in arm_StO_2 because only a percent (25% or 30%) of the 1% SpO_2 desaturation can contribute to StO_2 desaturation according to Formula (1). Thus, similar to the results of $finger_OD$ in response to CPAP titration shown in Table 2, arm_OD should also decrease stepwise with increasing CPAP pressures. However, the lack of correlation between the changes in $finger_OD$ and arm_OD and the missing association between CPAP pressures and arm_OD contradict this assumption, suggesting the fixed AVR model is unlikely to be valid in OSA. In fact, an OSA event is actually associated with increased vasoconstriction in peripheral limb arteries and arterioles [68,69], which suggests the AVR in the arm muscle is hardly constant during OSA. Most likely, coefficient a decreases while coefficient b increases in OSA because: (1) $a + b = 1$, and thus an increase in one coefficient must be associated with a decrease in the other, and arterial vessels have a stronger capacity to constrict than venous vessels; and (2) it is known that blood pressure, HR, left ventricular stroke volume and cardiac preload all decrease during apnea/hypopnea events [51,68,70–72], indicating more blood may be held in the venous vascular bed. Therefore, the contribution of venous blood to StO_2 increases while arterial blood contribution decreases during OSA events, leading to a reduction in the sensitivity of StO_2 in response to SpO_2 changes. This interpretation also fits our results that arm_OD has a negative association with the mean HR during the events (Table 1), i.e., a higher HR may indicate less vasoconstriction (i.e., relative larger a) and relatively more arterial blood supply to the muscle tissues; ergo arm_OD is smaller.

To the best of our knowledge, NIRS has not been used to measure the peripheral hemodynamics (i.e., muscular hemodynamics) in OSA. Our results of no correlation between the amplitudes of $finger_OD$ and arm_OD and the aforementioned increased venous contribution to StO_2 during OSA events indicate that our arm_OD measured by NIRS is likely to mainly represent the OD in venous blood. Our results (Tables 1 and 2) thus provide new insights into the changes in peripheral oxygen desaturation in OSA events during CPAP that (1) the arterial but not venous desaturation is more sensitive to changes in CPAP pressure; (2) arterial but not venous desaturation depends on the types of events (i.e., apnea causes larger desaturation than hypopnea) and sleep stages (light sleep causes larger desaturation than others); and (3) longer events cause larger desaturations in both arterial and venous blood as indicated by longer hypoxia that causes stronger oxygen extraction from both arterial and venous vascular bed.

In our recent study using the same database, we reported poor agreement (analyzed by Bland–Altman plots) between arm_OD and $finger_OD$ in sleep hypopneas, and thus the reliability of the AHI measured by StO_2 desaturation using wearable or portable optical sensors based on the NIRS technique is questionable [32]. This conclusion could be extended to wearable optical sensors based on an R-PPG technique such as wrist smartwatches because they face the same problem of venous blood influence as NIRS [32]. A recent study tested the accuracy of a wrist R-PPG smartwatch in measuring SpO_2 when SaO_2 measured from blood samples with a co-oximeter changed from 100% to 70% [73]. In that study, the Bland–Altman plot gave broad 95% lower (i.e., approximate –4%) and upper (i.e., approximate 6–7%) limits of agreement between smartwatch and co-oximeter measurements, which are similar to those reported in our study [32]. The authors also showed that the SpO_2 measurement error of their smartwatch is 3% [73]. This accuracy is still too poor to measure sleep hypopneas because hypopnea is defined as $\geq 3\%$ OD. Our results do not support the hypothesis that CPAP titration effectiveness may be assessed

by measuring peripheral StO₂ desaturation. This conclusion probably can apply to SpO₂ measured by smartwatches too.

Our study has several limitations. First, our patients may only represent male patients with severe OSA because although their age (Shapiro–Wilk normality test: p -value = 0.45) and BMI (Shapiro–Wilk normality test: p -value = 0.66) follow normal distribution, only three females were included. Whether our conclusions can be generated to females and patients with moderate OSA needs further studies. Second, correlation and association are not causality. Although we controlled multiple covariates (e.g., HR, sleep stages) in our LMM models, the causal relationships between CPAP pressures and changes in oxygen saturations in fingertip and arm muscle need further studies, e.g., studies with randomized CPAP pressures and/or multi-parameter (e.g., blood flow, endothelium function) measurements in addition to oxygen saturation. The causality analysis can essentially provide new insights into the hemodynamic regulations and consequences of CPAP therapy in OSA [74,75].

5. Conclusions

Although the recent boom of wearable optical sensors, such as smartwatches and armbands, offers a possibility of assessing OSA and multiple-night CPAP titrations at home, our negative results should warn the general public and sleep researchers/clinicians to be cautious with these wearable devices until those products are clinically and experimentally validated. More sophisticated algorithms such as machine learning are probably needed to derive some peripheral parameters that can correctly measure SpO₂ using wearable devices. Our results also suggest that the muscular StO₂ desaturation measured by NIRS may primarily represent venous desaturation in OSA. We suggest that more studies including the gold-standard invasive measurements of SaO₂ and SvO₂ together with simultaneous non-invasive NIRS measurement during OSA events are needed to further test the robustness and reliability of NIRS as a non-invasive tool in measuring SvO₂ in OSA.

Author Contributions: Conceptualization, Z.Z. and R.K.; Data curation, Z.Z., M.Q. and G.H.; Formal analysis, Z.Z.; Funding acquisition, Z.Z. and R.K.; Investigation, Z.Z., M.Q., G.H. and R.K.; Methodology, Z.Z.; Project administration, Z.Z. and R.K.; Resources, Z.Z. and R.K.; Software, Z.Z.; Supervision, R.K.; Validation, Z.Z. and R.K.; Visualization, Z.Z.; Writing—original draft, Z.Z.; Writing—review and editing, Z.Z. and R.K. All authors have read and agreed to the published version of the manuscript.

Funding: This work was supported by the Clinic Barmelweid Scientific Foundation. The data acquisition work was supported by the Research Fund of the Swiss Lung Association No. 2014–22.

Institutional Review Board Statement: The study was conducted according to the guidelines of the Declaration of Helsinki and approved by the local ethical commission of Northwest Switzerland.

Informed Consent Statement: Written informed consent to publish this paper was obtained from the patients.

Data Availability Statement: The raw data supporting the conclusions of this article are available from the corresponding author upon reasonable request.

Conflicts of Interest: The authors declare no conflict of interest.

References

1. Senaratna, C.V.; Perret, J.L.; Lodge, C.J.; Lowe, A.J.; Campbell, B.E.; Matheson, M.C.; Hamilton, G.S.; Dharmage, S.C. Prevalence of obstructive sleep apnea in the general population: A systematic review. *Sleep Med. Rev.* **2017**, *34*, 70–81. [[CrossRef](#)] [[PubMed](#)]
2. Yaggi, H.K.; Concato, J.; Kernan, W.N.; Lichtman, J.H.; Brass, L.M.; Mohsenin, V. Obstructive sleep apnea as a risk factor for stroke and death. *N. Engl. J. Med.* **2005**, *353*, 2034–2041. [[CrossRef](#)] [[PubMed](#)]
3. Somers, V.K. Sleep—A new cardiovascular frontier. *N. Engl. J. Med.* **2005**, *353*, 2070–2073. [[CrossRef](#)] [[PubMed](#)]
4. Lembo, D.; Caroccia, F.; Lopes, C.; Moscagiuri, F.; Sinjari, B.; D’Attilio, M. Obstructive Sleep Apnea and Periodontal Disease: A Systematic Review. *Medicina* **2021**, *57*, 640. [[CrossRef](#)]
5. Botros, N.; Concato, J.; Mohsenin, V.; Selim, B.; Doctor, K.; Yaggi, H.K. Obstructive sleep apnea as a risk factor for type 2 diabetes. *Am. J. Med.* **2009**, *122*, 1122–1127. [[CrossRef](#)] [[PubMed](#)]
6. Calik, M.W. Treatments for Obstructive Sleep Apnea. *J. Clin. Outcomes Manag.* **2016**, *23*, 181–192. [[PubMed](#)]

7. Sharma, S.K.; Agrawal, S.; Damodaran, D.; Sreenivas, V.; Kadiravan, T.; Lakshmy, R.; Jagia, P.; Kumar, A. CPAP for the metabolic syndrome in patients with obstructive sleep apnea. *N. Engl. J. Med.* **2011**, *365*, 2277–2286. [CrossRef]
8. Basner, R.C. Continuous positive airway pressure for obstructive sleep apnea. *N. Engl. J. Med.* **2007**, *356*, 1751–1758. [CrossRef]
9. Randerath, W.; Bassetti, C.L.; Bonsignore, M.R.; Farre, R.; Ferini-Strambi, L.; Grote, L.; Hedner, J.; Kohler, M.; Martinez-Garcia, M.A.; Mihaicuta, S.; et al. Challenges and perspectives in obstructive sleep apnoea: Report by an ad hoc working group of the Sleep Disordered Breathing Group of the European Respiratory Society and the European Sleep Research Society. *Eur. Respir. J.* **2018**, *52*, 1702616. [CrossRef]
10. Penzel, T.; Schobel, C.; Fietze, I. New technology to assess sleep apnea: Wearables, smartphones, and accessories. *F1000Research* **2018**, *7*, 413. [CrossRef]
11. Young, T.; Evans, L.; Finn, L.; Palta, M. Estimation of the clinically diagnosed proportion of sleep apnea syndrome in middle-aged men and women. *Sleep* **1997**, *20*, 705–706. [CrossRef] [PubMed]
12. Flemons, W.W.; Douglas, N.J.; Kuna, S.T.; Rodenstein, D.O.; Wheatley, J. Access to diagnosis and treatment of patients with suspected sleep apnea. *Am. J. Respir. Crit. Care Med.* **2004**, *169*, 668–672. [CrossRef]
13. Santilli, M.; Manciocchi, E.; D’Addazio, G.; Di Maria, E.; D’Attilio, M.; Femminella, B.; Sinjari, B. Prevalence of Obstructive Sleep Apnea Syndrome: A Single-Center Retrospective Study. *Int. J. Environ. Res. Public Health* **2021**, *18*, 277. [CrossRef] [PubMed]
14. Drager, L.F. New Challenges for Sleep Apnea Research: Simple Diagnostic Tools, Biomarkers, New Treatments and Precision Medicine. *Sleep Sci.* **2017**, *10*, 55–56. [CrossRef]
15. Fitbit. How Do I Track My Estimated Oxygen Variation in the Fitbit App? Available online: https://help.fitbit.com/articles/en_US/Help_article/1876.htm (accessed on 8 July 2021).
16. Garmin. Pulse Ox Frequently Asked Questions for Garmin Watches. Available online: <https://support.garmin.com/en-US/?faq=SK2Y9a9aBp5D6n4sXmPBG7> (accessed on 8 July 2021).
17. Huami. Amazfit X Bow to the Future. Available online: <https://www.amazfit.com/en/amazfit-x.html> (accessed on 8 July 2021).
18. Huawei. Huawei Watch 3. Available online: <https://consumer.huawei.com/en/wearables/watch-3/> (accessed on 8 July 2021).
19. Humon. Humon Muscle Oxygen Sensor. Available online: <https://humon.io/> (accessed on 8 July 2021).
20. Farzam, P.; Starkweather, Z.; Franceschini, M.A. Validation of a novel wearable, wireless technology to estimate oxygen levels and lactate threshold power in the exercising muscle. *Physiol. Rep.* **2018**, *6*, e13664. [CrossRef] [PubMed]
21. Moxy. The Science Behind Moxy. Available online: http://www.moxymonitor.com/wp-content/themes/moxymonitor/documents/Moxy_Scientific_Explanation_march2014.pdf (accessed on 8 July 2021).
22. Feldmann, A.; Schmitz, R.; Erlacher, D. Near-infrared spectroscopy-derived muscle oxygen saturation on a 0% to 100% scale: Reliability and validity of the Moxy Monitor. *J. Biomed. Opt.* **2019**, *24*, 1–11. [CrossRef] [PubMed]
23. Artinis. PortaMon. Available online: <https://www.artinis.com/portamon> (accessed on 8 July 2021).
24. Biofourmis, A.G. What Does the Everion Measure? Available online: <https://support.biofourmis.com/hc/en-us/articles/213613165-What-does-the-Everion-measure> (accessed on 8 July 2021).
25. Villringer, A.; Chance, B. Non-invasive optical spectroscopy and imaging of human brain function. *Trends Neurosci.* **1997**, *20*, 435–442. [CrossRef]
26. Delpy, D.T.; Cope, M.; van der Zee, P.; Arridge, S.; Wray, S.; Wyatt, J. Estimation of optical pathlength through tissue from direct time of flight measurement. *Phys. Med. Biol.* **1988**, *33*, 1433–1442. [CrossRef] [PubMed]
27. Scholkmann, F.; Kleiser, S.; Metz, A.J.; Zimmermann, R.; Mata Pavia, J.; Wolf, U.; Wolf, M. A review on continuous wave functional near-infrared spectroscopy and imaging instrumentation and methodology. *Neuroimage* **2014**, *85 Pt 1*, 6–27. [CrossRef]
28. Chan, E.D.; Chan, M.M. Pulse oximetry: Understanding its basic principles facilitates appreciation of its limitations. *Respir. Med.* **2013**, *107*, 789–799. [CrossRef]
29. König, V.; Huch, R.; Huch, A. Reflectance Pulse Oximetry—Principles and Obstetric Application in the Zurich System. *J. Clin. Monit. Comput.* **1998**, *14*, 403–412. [CrossRef] [PubMed]
30. Nitzan, M.; Romem, A.; Koppel, R. Pulse oximetry: Fundamentals and technology update. *Med. Devices (Auckl. N. Z.)* **2014**, *7*, 231–239. [CrossRef] [PubMed]
31. Menghini, L.; Cellini, N.; Goldstone, A.; Baker, F.C.; de Zambotti, M. A standardized framework for testing the performance of sleep-tracking technology: Step-by-step guidelines and open-source code. *Sleep* **2021**, *44*, zsa170. [CrossRef] [PubMed]
32. Zhang, Z.; Qi, M.; Hugli, G.; Khatami, R. The Challenges and Pitfalls of Detecting Sleep Hypopnea Using a Wearable Optical Sensor: Comparative Study. *J. Med. Internet Res.* **2021**, *23*, e24171. [CrossRef] [PubMed]
33. Berry, R.B.; Kushida, C.A.; Kryger, M.H.; Soto-Calderon, H.; Staley, B.; Kuna, S.T. Respiratory event detection by a positive airway pressure device. *Sleep* **2012**, *35*, 361–367. [CrossRef]
34. Kim, D.E.; Hwangbo, Y.; Bae, J.H.; Yang, K.I. Accuracy of residual apnea-hypopnea index obtained using the continuous positive airway pressure device: Application of new version 2.0 scoring rules for respiratory events during sleep. *Sleep Breath.* **2015**, *19*, 1335–1341. [CrossRef]
35. Stepnowsky, C.; Zamora, T.; Barker, R.; Liu, L.; Sarmiento, K. Accuracy of positive airway pressure device-measured apneas and hypopneas: Role in treatment followup. *Sleep Disord.* **2013**, *2013*, 314589. [CrossRef]
36. Weaver, T.E.; Sawyer, A.M. Adherence to continuous positive airway pressure treatment for obstructive sleep apnoea: Implications for future interventions. *Indian J. Med. Res.* **2010**, *131*, 245–258.
37. Wolk, R.; Shamsuzzaman, A.S.; Somers, V.K. Obesity, sleep apnea, and hypertension. *Hypertension* **2003**, *42*, 1067–1074. [CrossRef]

38. Watzman, H.M.; Kurth, C.D.; Montenegro, L.M.; Rome, J.; Steven, J.M.; Nicolson, S.C. Arterial and venous contributions to near-infrared cerebral oximetry. *Anesthesiology* **2000**, *93*, 947–953. [[CrossRef](#)]
39. Franceschini, M.A.; Thaker, S.; Themelis, G.; Krishnamoorthy, K.K.; Bortfeld, H.; Diamond, S.G.; Boas, D.A.; Arvin, K.; Grant, P.E. Assessment of infant brain development with frequency-domain near-infrared spectroscopy. *Pediatr. Res.* **2007**, *61*, 546–551. [[CrossRef](#)]
40. Berry, R.B.; Brooks, R.; Gamaldo, C.E.; Harding, S.M.; Lloyd, R.M.; Marcus, C.L.; Vaughn, B.V. *The AASM Manual for the Scoring of Sleep and Associated Events: Rules, Terminology and Technical Specifications*; American Academy of Sleep Medicine: Darien, IL, USA, 2017.
41. Fantini, S.; Sassaroli, A. Frequency-Domain Techniques for Cerebral and Functional Near-Infrared Spectroscopy. *Front. Neurosci.* **2020**, *14*, 300. [[CrossRef](#)] [[PubMed](#)]
42. Fantini, S.; Franceschini, M.-A.; Maier, J.S.; Walker, S.A.; Barbieri, B.B.; Gratton, E. Frequency-domain multichannel optical detector for noninvasive tissue spectroscopy and oximetry. *Opt. Eng.* **1995**, *34*, 32–42. [[CrossRef](#)]
43. Toronov, V.; Webb, A.; Choi, J.H.; Wolf, M.; Safonova, L.; Wolf, U.; Gratton, E. Study of local cerebral hemodynamics by frequency-domain near-infrared spectroscopy and correlation with simultaneously acquired functional magnetic resonance imaging. *Opt. Express* **2001**, *9*, 417–427. [[CrossRef](#)] [[PubMed](#)]
44. Fantini, S.; Franceschini, M.A.; Fishkin, J.B.; Barbieri, B.; Gratton, E. Quantitative determination of the absorption spectra of chromophores in strongly scattering media: A light-emitting-diode based technique. *Appl. Opt.* **1994**, *33*, 5204–5213. [[CrossRef](#)] [[PubMed](#)]
45. Kleiser, S.; Nasserli, N.; Andresen, B.; Greisen, G.; Wolf, M. Comparison of tissue oximeters on a liquid phantom with adjustable optical properties. *Biomed. Opt. Express* **2016**, *7*, 2973–2992. [[CrossRef](#)] [[PubMed](#)]
46. Stankovic, M.R.; Maulik, D.; Rosenfeld, W.; Stubblefield, P.G.; Kofinas, A.D.; Drexler, S.; Nair, R.; Franceschini, M.A.; Hueber, D.; Gratton, E.; et al. Real-time optical imaging of experimental brain ischemia and hemorrhage in neonatal piglets. *J. Perinat. Med.* **1999**, *27*, 279–286. [[CrossRef](#)] [[PubMed](#)]
47. Fantini, S.; Franceschini, M.; Gratton, E.; Hueber, D.; Rosenfeld, W.; Maulik, D.; Stubblefield, P.; Stankovic, M. Non-invasive optical mapping of the piglet brain in real time. *Opt. Express* **1999**, *4*, 308–314. [[CrossRef](#)] [[PubMed](#)]
48. Hallacoglu, B.; Sassaroli, A.; Wysocki, M.; Guerrero-Berrea, E.; Schnaider Beerli, M.; Haroutunian, V.; Shaul, M.; Rosenberg, I.H.; Troen, A.M.; Fantini, S. Absolute measurement of cerebral optical coefficients, hemoglobin concentration and oxygen saturation in old and young adults with near-infrared spectroscopy. *J. Biomed. Opt.* **2012**, *17*, 081401–081406. [[CrossRef](#)]
49. Fantini, S.; Hueber, D.; Franceschini, M.A.; Gratton, E.; Rosenfeld, W.; Stubblefield, P.G.; Maulik, D.; Stankovic, M.R. Non-invasive optical monitoring of the newborn piglet brain using continuous-wave and frequency-domain spectroscopy. *Phys. Med. Biol.* **1999**, *44*, 1543–1563. [[CrossRef](#)] [[PubMed](#)]
50. Kleiser, S.; Ostojic, D.; Andresen, B.; Nasserli, N.; Isler, H.; Scholkmann, F.; Karen, T.; Greisen, G.; Wolf, M. Comparison of tissue oximeters on a liquid phantom with adjustable optical properties: An extension. *Biomed. Opt. Express* **2018**, *9*, 86–101. [[CrossRef](#)] [[PubMed](#)]
51. Zhang, Z.; Schneider, M.; Laures, M.; Qi, M.; Khatami, R. The Comparisons of Cerebral Hemodynamics Induced by Obstructive Sleep Apnea with Arousal and Periodic Limb Movement with Arousal: A Pilot NIRS Study. *Front. Neurosci.* **2016**, *10*, 403. [[CrossRef](#)]
52. Zhang, Z.; Khatami, R. Predominant endothelial vasomotor activity during human sleep: A near-infrared spectroscopy study. *Eur. J. Neurosci.* **2014**, *40*, 3396–3404. [[CrossRef](#)] [[PubMed](#)]
53. Cleveland, W.S.; Devlin, S.J. Locally Weighted Regression—An Approach to Regression-Analysis by Local Fitting. *J. Am. Stat. Assoc.* **1988**, *83*, 596–610. [[CrossRef](#)]
54. Nakagawa, S.; Schielzeth, H. A general and simple method for obtaining R² from generalized linear mixed-effects models. *Methods Ecol. Evol.* **2013**, *4*, 133–142. [[CrossRef](#)]
55. Xu, R. Measuring explained variation in linear mixed effects models. *Stat. Med.* **2003**, *22*, 3527–3541. [[CrossRef](#)]
56. Kandel, G.; Aberman, A. Mixed venous oxygen saturation. Its role in the assessment of the critically ill patient. *Arch. Intern. Med.* **1983**, *143*, 1400–1402. [[CrossRef](#)]
57. Benni, P.B.; MacLeod, D.; Ikeda, K.; Lin, H.M. A validation method for near-infrared spectroscopy based tissue oximeters for cerebral and somatic tissue oxygen saturation measurements. *J. Clin. Monit. Comput.* **2018**, *32*, 269–284. [[CrossRef](#)] [[PubMed](#)]
58. Kreeger, R.N.; Ramamoorthy, C.; Nicolson, S.C.; Ames, W.A.; Hirsch, R.; Peng, L.F.; Glatz, A.C.; Hill, K.D.; Hoffman, J.; Tomasson, J.; et al. Evaluation of pediatric near-infrared cerebral oximeter for cardiac disease. *Ann. Thorac. Surg.* **2012**, *94*, 1527–1533. [[CrossRef](#)] [[PubMed](#)]
59. Bickler, P.E.; Feiner, J.R.; Rollins, M.D. Factors affecting the performance of 5 cerebral oximeters during hypoxia in healthy volunteers. *Anesth. Analg.* **2013**, *117*, 813–823. [[CrossRef](#)] [[PubMed](#)]
60. Henson, L.C.; Calalang, C.; Temp, J.A.; Ward, D.S. Accuracy of a cerebral oximeter in healthy volunteers under conditions of isocapnic hypoxia. *Anesthesiology* **1998**, *88*, 58–65. [[CrossRef](#)]
61. Shah, N.; Trivedi, N.K.; Clack, S.L.; Shah, M.; Shah, P.P.; Barker, S. Impact of hypoxemia on the performance of cerebral oximeter in volunteer subjects. *J. Neurosurg. Anesthesiol.* **2000**, *12*, 201–209. [[CrossRef](#)]

62. Benni, P.B.; Chen, B.; Dykes, F.D.; Wagoner, S.F.; Heard, M.; Tanner, A.J.; Young, T.L.; Rais-Bahrami, K.; Rivera, O.; Short, B.L. Validation of the CAS neonatal NIRS system by monitoring vv-ECMO patients: Preliminary results. *Adv. Exp. Med. Biol.* **2005**, *566*, 195–201. [[CrossRef](#)] [[PubMed](#)]
63. Rais-Bahrami, K.; Rivera, O.; Short, B.L. Validation of a noninvasive neonatal optical cerebral oximeter in veno-venous ECMO patients with a cephalad catheter. *J. Perinatol.* **2006**, *26*, 628–635. [[CrossRef](#)] [[PubMed](#)]
64. Ikeda, K.; MacLeod, D.B.; Grocott, H.P.; Moretti, E.W.; Ames, W.; Vacchiano, C. The accuracy of a near-infrared spectroscopy cerebral oximetry device and its potential value for estimating jugular venous oxygen saturation. *Anesth. Analg.* **2014**, *119*, 1381–1392. [[CrossRef](#)] [[PubMed](#)]
65. Redford, D.; Paidy, S.; Kashif, F. Absolute and trend accuracy of a new regional oximeter in healthy volunteers during controlled hypoxia. *Anesth. Analg.* **2014**, *119*, 1315–1319. [[CrossRef](#)] [[PubMed](#)]
66. Franceschini, M.A.; Boas, D.A.; Zourabian, A.; Diamond, S.G.; Nadgir, S.; Lin, D.W.; Moore, J.B.; Fantini, S. Near-infrared spirometry: Noninvasive measurements of venous saturation in piglets and human subjects. *J. Appl. Physiol.* **2002**, *92*, 372–384. [[CrossRef](#)]
67. MacDonald, M.J.; Tarnopolsky, M.A.; Green, H.J.; Hughson, R.L. Comparison of femoral blood gases and muscle near-infrared spectroscopy at exercise onset in humans. *J. Appl. Physiol.* **1999**, *86*, 687–693. [[CrossRef](#)] [[PubMed](#)]
68. Imadojemu, V.A.; Gleeson, K.; Gray, K.S.; Sinoway, L.I.; Leuenberger, U.A. Obstructive apnea during sleep is associated with peripheral vasoconstriction. *Am. J. Respir. Crit. Care Med.* **2002**, *165*, 61–66. [[CrossRef](#)] [[PubMed](#)]
69. Kraiczi, H.; Hedner, J.; Peker, Y.; Carlson, J. Increased vasoconstrictor sensitivity in obstructive sleep apnea. *J. Appl. Physiol.* **2000**, *89*, 493–498. [[CrossRef](#)]
70. Smith, R.P.; Veale, D.; Pepin, J.L.; Levy, P.A. Obstructive sleep apnoea and the autonomic nervous system. *Sleep Med. Rev.* **1998**, *2*, 69–92. [[CrossRef](#)]
71. Andreas, S.; Hajak, G.; von Breska, B.; Ruther, E.; Kreuzer, H. Changes in heart rate during obstructive sleep apnoea. *Eur. Respir. J.* **1992**, *5*, 853–857. [[PubMed](#)]
72. Tolle, F.A.; Judy, W.V.; Yu, P.L.; Markand, O.N. Reduced stroke volume related to pleural pressure in obstructive sleep apnea. *J. Appl. Physiol. Respir. Environ. Exerc. Physiol.* **1983**, *55*, 1718–1724. [[CrossRef](#)] [[PubMed](#)]
73. Kirszenblat, R.; Edouard, P. Validation of the Withings ScanWatch as a Wrist-Worn Reflective Pulse Oximeter: Prospective Interventional Clinical Study. *J. Med. Internet Res.* **2021**, *23*, e27503. [[CrossRef](#)]
74. Reichmuth, K.J.; Dopp, J.M.; Barcsi, S.R.; Skatrud, J.B.; Wojdyla, P.; Hayes, D., Jr.; Morgan, B.J. Impaired vascular regulation in patients with obstructive sleep apnea: Effects of continuous positive airway pressure treatment. *Am. J. Respir. Crit. Care Med.* **2009**, *180*, 1143–1150. [[CrossRef](#)]
75. Spicuzza, L.; Bernardi, L.; Balsamo, R.; Ciancio, N.; Polosa, R.; Di Maria, G. Effect of treatment with nasal continuous positive airway pressure on ventilatory response to hypoxia and hypercapnia in patients with sleep apnea syndrome. *Chest* **2006**, *130*, 774–779. [[CrossRef](#)] [[PubMed](#)]